The optimal design and operation of a hybrid renewable micro-grid with the decoupled liquid air energy storage

Liang, Ting; Webley, Paul A.; Chen, Yi Chung; She, Xiaohui; Li, Yongliang; Ding, Yulong

DOI:
10.1016/j.jclepro.2021.130189

Document Version
Peer reviewed version

Citation for published version (Harvard):
Liang, T, Webley, PA, Chen, YC, She, X, Li, Y & Ding, Y 2022, 'The optimal design and operation of a hybrid renewable micro-grid with the decoupled liquid air energy storage', *Journal of Cleaner Production*, vol. 334, 130189. https://doi.org/10.1016/j.jclepro.2021.130189

The optimal design and operation of a hybrid renewable micro-grid with the decoupled liquid air energy storage

Ting Liang[a*], Paul A. Webley[b], Yi-Chung Chen[a], Xiaohui She[a,c], Yongliang Li[a], Yulong Ding[a*]

a Birmingham Centre for Energy Storage, School of Chemical Engineering, University of Birmingham, Birmingham B15 2TT, UK

b Department of Chemical Engineering, Monash Universimty, Building 94, Clayton Campus, Australia

c School of Mechanical Engineering, Shijiazhuang Tiedao University, Shijiazhuang 050043, China

txl880@student.bham.ac.uk; y.ding@bham.ac.uk (Corresponding Authors)

Keywords: Hybrid renewable micro-grid, decoupled liquid air energy storage, optimal energy to power ratio, storage value breakdown, optimal design and operation, mixed-integer linear programming

Abbreviations		**Subscripts**	
CHP	Combined heat and power	*hex*	Heat exchanger
CAES	Compressed air energy storage	*i*	The i^{th} equipment
Cha E/P	Charge energy/power ratio	*j*	The j^{th} equipment candidate
Dis E/P	Discharge energy/power ratio	*z*	The z^{th} renewable energy
EC	Electric chiller	0	Reference parameters
ESS	Energy storage system	+	Output power (storage)
FIT	Feed-in tariff	-	Absorb power (storage)
GE	Gas engine		
GB	Gas boiler		
HS	Heat storage		
HRMG	Hybrid renewable micro-grid	**Symbols**	
HRES	Hybrid renewable energy system	*a*/*b*/*p*/*q*	Regression coefficients
HP	Heat pumps	A	Area [m2]
LAES	Liquid air energy storage	*Amf*	Amortized factor
LOA	Level of liquid air	$\boldsymbol{A}$	Constraints matrix for continuous variables
LOP	Loss of power	$\boldsymbol{Ax}$	Auxiliary variable vector
MES	Multi-vector energy system	$\boldsymbol{b}$	Known-term vector
MILP	Mixed-integer linear programming	$\boldsymbol{B}$	Constraints matrix for binary variables
NG	Natural gas	*C1*	Constant 1
LOLE	Loss of load expectation	*C2*	Constant 2
LFU	Liquefaction unit	CF	Capacity factor [kW]
O&M	Operation & Maintenance	C_z	The z^{th} cost component [£]
PV	Photovoltaic	$\boldsymbol{c}$	Cost matrix for continuous variables
PRU	Power recovery unit	$\boldsymbol{d}$	Cost matrix for binary variables
PID	Proportion, Integration, Differentiation	$\boldsymbol{Des}$	Design variable set
PSO	Particle swarm optimization	*ems*	Emission of CO_2 [kg/kWh]
PHS	Pump hydro storage	*emf*	Emission factor [kg CO_2/kg]
ROI	Return on investment	*E*	Energy capacity [kWh]

RTE	Round trip efficiency	h	Enthalpy [kJ/kg]
RP	Ratio of power	$\boldsymbol{I}$	Design variable space
RM	Ratio of mass flow rate	$\boldsymbol{J}$	Auxiliary variable space
STOR	Short term operating reserve	IR	Interest rate
Subscripts		k	Slope coefficient
ava	Available	Lf	Lifetime [years]
ann	Annual	$\dot{m}$	Mass flow rate [kg/s]
amb	Ambience	$\boldsymbol{M}$	Mode vector of heat pump
bat	Battery	$\boldsymbol{N}$	Selected number vector
C	Compressor	n	Selected number
cur	Curtailment	N	Turbine speed
col	Cooling	Nx	Dimension of continuous variables
cpt	Capital cost	Ny	Dimension of binary variable
capa	Capacity	$\boldsymbol{of}$	On_off status matrix
cha	Charge	$\boldsymbol{of\_num}$	On_off number matrix
dis	Discharge	*online*	Online status of equipment
dn	Ramp down	OR	Operating reserve
ep	Equipment	P	Electricity power [kW]
ele	Electricity	Pr	Price [£/kWh]
f	Fuel	Q_h	Heat power [kW]
grid	Electricity grid	Q_f	Fuel power [kW]
gs	Gas	R	Real number set
ht	Heat	RP	Ratio of power
inc	Incentive	RM	Ratio of mass flow rate
los	Loss	$\boldsymbol{S}$	Selection number set
L	Load	*SOC*	Storage level
LA	Liquid air	t	Time
min	Minimum value	$\boldsymbol{T}$	Time domain
max	Maximum value	Tax	CO_2 tax [£/kg]
main	Maintenance	V	Volume [m^3]
in	Inlet parameters	$\boldsymbol{Z}$	Integer set
o	outlet parameters	η	Mechanical efficiency
op	Operation cost	β	Expansion ratio
r	Rated power	ρ	Density [kg/m^3]
rh	Recoverable heat	‘	Normalized parameters
rew	Renewable	¯	Reduced parameters
ST	Storage	$\boldsymbol{x}$	Continuous variable vector
Tr	Expansion turbines	$\boldsymbol{y}$	Binary variable vector
tot	Total		
pv	Photovoltaic		
wt	Wind turbines		
up	Ramp up		

1 Introduction

Recent years have seen a growing interest in developing distributed hybrid renewable energy systems (HRESs) (Jihane Kartite, 2019). Such systems combine conventional generators with renewables to reduce carbon dioxide emissions. With an increasing depth of renewable deployment, energy storage would become essential for stabilizing and smoothing the intermittent outputs of renewables. This facilitates the decarbonisation of the energy sector, which accounts for over 70% of the greenhouse gas emissions (Vivien Foster, 2014). This work is concerned with the optimal design and operation of a hybrid renewable micro-grid with decoupled liquid air energy storage. A brief review of the most relevant work is given in the following.

Hybrid renewable energy system design methods

A few studies have investigated HRESs at different scales by using different methods. Based on a concept called 'energy hub', Geidl (2007) proposed a general steady-state modelling and optimization framework, involving the conversion, transmission and storage of energy with multiple carriers. Good et al. (2016) proposed a modular techno-economic model to study the physical and commercial interactions of different energy vectors within the HRES. Ayele et al. (2019) developed a load flow model based on an extended energy hub approach, and used a nested particle swarm optimization (NPSO) algorithm for the optimisation. Buonomano et al. (2014) designed a new HRES and carried out a techno-economic analysis in the TRNSYS (Transient System Simulation) environment. Zakeri et al. (2015) adopted the EnergyPLAN to investigate the maximum penetration ratio of different renewables and the optimal combination of different technologies. A new methodology for designing an off-grid hybrid PV-diesel-battery system was developed (Mokhtara et al., 2020), which combines demand-supply management (DSM) with particle swarm optimization. The results showed that PV-Li-ion was the optimal configuration, which could achieve 19% and 57% reduction in energy consumption and CO_2 emissions respectively. An overview about the design methodologies, components sizing and economic indicators of HRES was provided (Lian et al., 2019), pointing out that the hybrid methods are the most promising ones for designing HRES. A triple-hybrid vapour absorption cooling system powered by solar, natural gas and auxiliary electricity-based cogeneration was investigated, it showed a good potential to save electric energy consumption and cost (Singh and Das, 2018). The same authors also experimentally studied a small-scale triple-hybrid air-conditioning system powered by solar energy and biomass. The techno-economic analysis indicated a decent coefficient of performance (0.34) and a payback period of 9-12 years (Singh and Das, 2021).

MILP optimisation of hybrid renewable energy system

Although various design methods of HRESs have been outlined above, the mixed-integer linear programming (MILP) has been one of the most popular and powerful tools for the optimal design and operation of HRESs. This is due to its moderate complexity and ability

to achieve the global optimal point. Yokoyama et al. (2015) proposed a hierarchical MILP method for the optimal design and scheduling of a poly-generation system. It showed a higher efficiency but the same accuracy when compared with the conventional MILP method. Yang et al. (2015) constructed a MILP model for a distributed energy system, which can achieve the optimization of resource locations, technology combination and operation strategies. F. J. de Sisternes (2013) developed a MILP-based extended Investment Model for Renewable Electricity Systems (IMRES). It is used for exploring the potential value of energy storage in decarbonizing the electricity sector, but the complementary characteristics of energy storage technologies were not considered. Arcuri et al. (2007) proposed a MILP design and scheduling model for a tri-generation plant. They performed the short-term and long-term optimization for saving energy and cost, but they did not consider renewable energy in the system. A MILP method to optimally size a hybrid off-grid solar-wind system with battery storage was developed to replace diesel engines, but the input profiles were too simplified to represent a realistic scenario (Alberizzi et al., 2020). An author developed a two-stage MILP model to minimize the overall levelized cost for a standalone micro-grid. It was capable of determining the optimal selection and operation of system components, but the economic sensitivity analysis was not considered (Tu et al., 2019).

Hybrid renewable energy system with energy storage

As mentioned above, energy storage is essential for supporting the operation of HRESs. A number of studies have discussed the integration of different energy storage technologies with HRESs. This includes the pump hydro storage (PHS), the compressed air energy storage (CAES), the liquid air energy storage (LAES), the thermochemical and electrochemical energy storages. Djelailia et al. (2019) studied an HRES with PHS, it showed the effectiveness of hydroelectric storage in irrigation, power dispatch, fuel-saving and CO_2 emissions. de Bosio and Verda (2015) investigated a hybrid renewable power plant with CAES. The thermo-economic analysis indicated that the hybrid system would be cost-effective only when used to solve the grid imbalance. However, PHS and CAES considered in the studies have geographical limitations. Gabrielli et al. (2018) proposed a MILP-based model to optimally design a HRES with hydrogen storage, but this technology has a low technical maturity. Martínez Ceseña et al. (2018) conducted a techno-economic analysis of a micro-grid with battery storage and thermal energy storage. The storage technologies can provide energy, reserve, and reliability services simultaneously, but the flexibility value of storages was not considered. A comprehensive analysis of a novel system combining LAES and thermal storage was conducted. The system can obtain both high energy efficiency (61.1%) and exergy efficiency (52.8%), as well as a promising pay-back period of 3.91 years (Nabat et al., 2020). Mazzoni S. (2019) developed an MILP dispatch model to compare the economic performance of LAES and battery (300-2000 kWh), but the model cannot perform the optimal system design with LAES. Xie et al. (2018) assessed the economic value of a decoupled LAES system when participating in the UK electricity service markets. It showed that a large-scale LAES with

high-grade waste heat (>150 ℃) would be profitable, but the detailed technical data of LAES was not taken into account. Vecchi et al. (2020a) conducted a techno-economic analysis of a standalone LAES system within the UK electricity markets, considering the off-design operation. They also investigated the techno-economic value of LAES to supply electricity, heating and cooling functions simultaneously. The vector-coupling capability of LAES is capable of achieving a 35% of increase in energy efficiency and a 8-12% of decrease in system operational cost (Vecchi et al., 2021). However, the interactions of the gird-scale LAES system with other power generators were not studied.

Objectives of this study

From the above review, one can see little work has been done on the integration of LAES with hybrid renewable micro-grids (HRMGs), nor on the specific value streams of this storage technology. This makes it difficult to understand whether the deployment of LAES in distributed HRMGs would be feasible and valuable. The research questions were thus set for this work to answer: a) Is it possible to integrate small-scale LAESs with HRMGs to help manage the increasing renewable penetration? b) What are the specific value streams of LAESs when applied into HRMGs? What scenarios can greatly increase the attractiveness of LAESs in HRMGs? c) If it is of value, what are the optimal capacities of LAESs to be equipped to generate the best cost-effectiveness and environmental benefits in HRMGs? Thus, the goal of this work is to answer the questions above, which also fills the literature gaps identified above. This is done by investigating the value and optimal selection of LAESs to support future distributed micro-grids. The major contributions and novelties of this work lie in the following four aspects:

- The decoupled off-design LAES model is developed, which can adapt to the fluctuating renewables and variable user demands, as well as can achieve the optimal selection of LAES units in a HRMG by using the MILP algorithm.
- The optimal charge and discharge energy to power (E/P) ratios of LAESs are studied for the first time when providing different electricity services. It enables preliminarily determining the LAES capacities when providing the arbitrage, renewable firming and operating reserve functions.
- The multiple functions and revenue streams of LAESs in supporting HRMGs are identified for the first time, which are split into different compositions. The interactions among different value streams are also discussed and compared with those of the battery storage.
- The optimal design and operation of a HRMG with the decoupled LAES by using the hierarchical MILP formulation is achieved for the first time. The optimal sizes and operational states of the decoupled LAES units and other generators can be determined, to incorporate a large portion of renewables with the minimum cost and environmental impact.

The paper is structured in the following manner. Section 2 describes the components' model and parameters. Section 3 introduces the input profiles and related input parameters. Section 4 presents the MILP methodology and modelling methods. The major results are explained in Section 5. Finally, conclusions are drawn in Section 6.

2 Case study and input definition

2.1 Hybrid renewable micro-grid

A future hybrid renewable micro-grid (HRMG) for the University of Birmingham campus is proposed as the case study, as shown in Fig. 1. It is to help achieve an independent demand supply with simultaneous economic savings and CO_2 reductions.

The HRMG is connected to the national grid and gas pipelines. It is composed of conventional technologies, like CHPs (combined heat and power technology), boilers and heat pumps (HP); and renewable-based generators, including wind turbines, solar PV and CSP (concentrated solar power); as well as energy storage systems (ESS), like LAES, battery, heat storage and cold storage. The goal is to reduce the total cost and CO_2 emissions. This work focuses on reducing at least 50% of CO_2 emissions on the 2016 level as the first-stage transition. The optimal design and operation framework of the HRMG is formulated as a hierarchical MILP model, in which LAES serves as one of the major electricity energy storages.

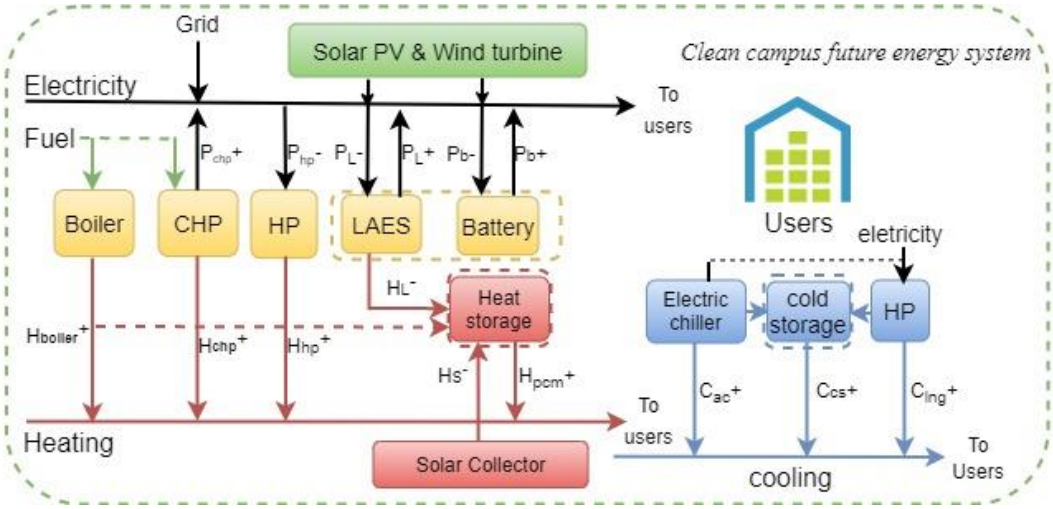

Fig. 1. Future HRMG scheme for the campus

2.2 Micro-grid components models

The LAES is composed of three major sub-systems, the air liquefaction unit (LFU), the air storage tank and the air power recovery unit (PRU), shown as in Fig. 2. The LFU absorb off-peak electricity from the grid or renewables to produce liquid air, which is stored in cryogenic tanks. The PRU produces electric power by consuming liquid air when electricity prices are high. The compression heat and high-grade cold energy can both be recovered to increase the system round trip efficiency (RTE). The decoupled LAES model is developed, in which the models of the LFU, PRU and storage tank are built separately and explained in detail in section 1.1 of the supplementary material. The models consider the off-design operation and RTE, the varying power consumption and production, as well as the decoupled costs of subsystems, to achieve good cost-effectiveness and practical assessment. The nominal

operating parameters of the LAES are presented in Table 1, with the optimal parameters chosen on the basis of thermodynamic analysis results reported by She. *et al.* (She et al., 2017).

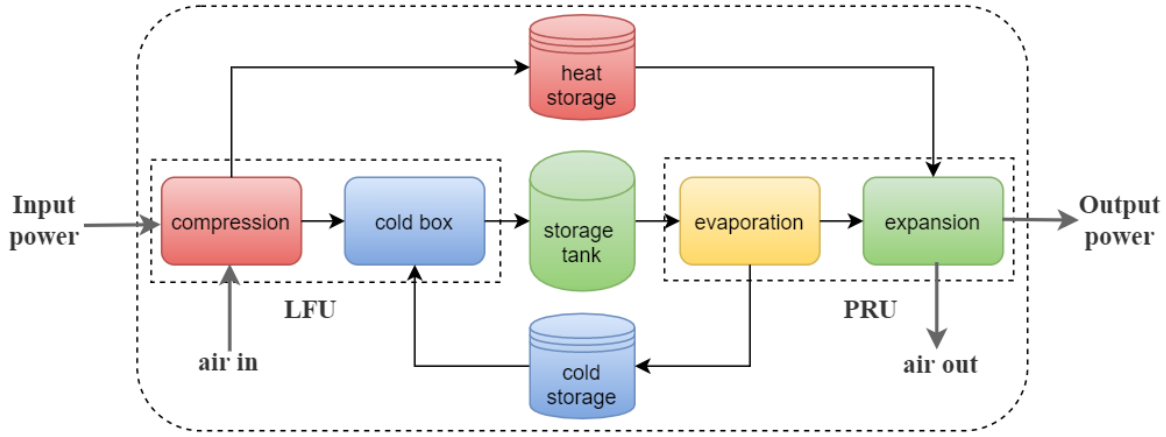

Fig. 2. The decoupled LAES system

Table 1. LAES nominal operating conditions

Nominal parameters	value
Charge pressure/MPa	10
Discharge pressure/MPa	10
Turbine inlet temperature / ℃	195
Liquefaction rate	70%
RTE	52.5%
Compressor efficiency	89%
Turbine efficiency	90%
Cryo-turbine efficiency	80%
Intercooler effectiveness	95%
Compression enthalpy kJ/kg	193.00
Expansion enthalpy kJ/kg	145.00

In the HRMG, other components, including the gas engines, heat pumps, electric chillers, gas boilers, battery, solar PV and wind turbines are contributing to providing energy for the campus micro-grid as well. Their models and key parameters are explained in section 1 of the supplementary material, summarized as in Table 2.

Table 2. Technical and economic parameters of other system components

Components	**Efficiency**	**Life time/years**	**Capital cost/£**	**O&M cost /% of CAPEX**
Gas engine	86% (total)	15	$6962.5 * Pr^{-0.164}$ /kW	0.05
Gas boiler	85%	20	80/kW	0.02
Electric chiller	2.8	15	$1164.2 \cdot P_r^{-0.284}$ /kW	0.015
Heat pumps	0.0329*T_{amb}+2.0012	15	$1319.4 \cdot P_r^{-0.268}$ /kW	0.015
Air compressor	85%	30	$Cost_{c0}(\frac{P_c}{P_{c0}})^{-0.4}$	0.01
Air turbine	85%	30	$Cost_{t0}(\frac{P_t}{P_{t0}})^{-0.4}$	0.01
Liquid air tank	/	30	44/kWh	0.01
Solar PV	16.67%	30	900/kW	3 /year/kW

Wind turbines	/	30	1300/kW	7.5/year/kW
Battery	95% (charge/discharge)	10	420/kWh	0.02
Heat storage	95% (charge/discharge)	20	10/kWh	0.02

2.3 Demand profiles

The campus of the University of Birmingham was chosen as the case study. Considering the significant complexity and calculation volume caused by full-scale optimization, the hourly profiles in four representative weeks in a year are chosen to represent four separate seasons. The profiles include: 1) the electricity, heating and cooling demands (shown in Fig. 3); 2) the solar and wind capacity factors; 3) the ambient temperature and unit-rate electricity prices. The methods to choose the representative data and profiles are illustrated in the section 2 of the supplementary material. The annual operational cost and revenue will be calculated by multiplying a weight factor (13) based on the simulation results of the representative weeks (Martínez Ceseña et al., 2018).

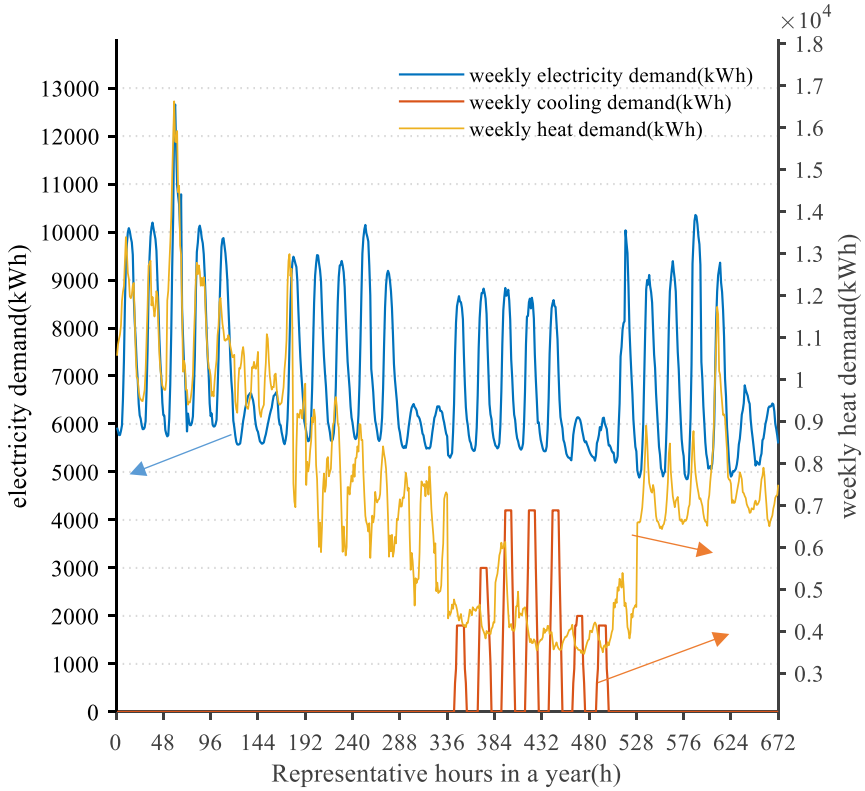

Fig. 3. Representative electricity/heat/cooling demands in campus

2.4 Input parameters

The campus micro-grid interacts with the national electricity grid, gas network, and other stakeholders. The input parameters of the model are explained in the section 2.1 and 2.2 of the supplementary material, summarized as in Table 3, including the retailing gas prices, renewable incentives, carbon emission factor and tax, loss of power and curtailment penalty, the search space of variables, and the performance indicators.

Table 3. Model input 'environment' parameters

Components	Parameters	Data	Unit
Energy bill	Gas bill rates	1.04 (summer) / 1.37 (spring) / 2.22 (winter)	p/kWh
	Electricity bill rates	-12 ~ 120 (valley ~ peak)	p/kWh
Incentives	Renewable heat	2.69	p/kWh
	Solar PV	1.78	p/kWh
	Wind power	0.88	p/kWh
Penalty	Wind curtailment penalty	80	£/MWh
	Loss of power penalty	17000	£/MWh
CO_2 related	NG CO_2 emission factor	185	kg/MWh
	Carbon price	18	£/t
Reserve related	Loss of load expectation (LOLE)	3	hours/year
	Reserve charge	0.83	£/kW

3 MILP method and formulation

3.1 MILP algorithm description

The optimal design and operation framework for the micro-grid is formulated as a hierarchical MILP model. It includes two levels, namely the upper design level and the lower operational level. The variables include: the binary variables to represent the selection value, integer variables represent the selected number, and continuous variables to represent design capacities and operational parameters. The model can be described in a general form in eq. (1)-(3) (Gabrielli et al., 2018).

$$\mathbf{min}(\boldsymbol{c^T x} + \boldsymbol{d^T y}) \quad (1)$$

$$\boldsymbol{Ax} + \boldsymbol{By} = \boldsymbol{b} \quad (2)$$

$$\boldsymbol{x} \geq \mathbf{0} \in \boldsymbol{R^{N_x}}, \boldsymbol{y} \in \{\mathbf{0}, \mathbf{1}\}^{N_y} \quad (3)$$

where, $\boldsymbol{x}$ represents continuous variable vector, $\boldsymbol{y}$ represents binary variable vector, $\boldsymbol{A}$ and $\boldsymbol{B}$ are the corresponding constraints matrices, and $\boldsymbol{b}$ is the constraint known-term vector; N_x and N_y represent the dimensions of $\boldsymbol{x}$ and $\boldsymbol{y}$. $\boldsymbol{c}$ and $\boldsymbol{d}$ represent the cost matrices for continuous and binary variables.

3.1.1 Decision variables

The decision variables are divided into three categories:

i. Design variables, including the selection value ($\boldsymbol{S} \in R^{\boldsymbol{I}}$), selected number ($\boldsymbol{N} \in Z^{\boldsymbol{I_{ep}}}$), and rated sizes of system components ($\boldsymbol{Des_{ep}} \in R^{\boldsymbol{I_{ep}}}$) and storage devices ($\boldsymbol{Des_{ST}} \in R^{\boldsymbol{I_{ST}}}$).

ii. Operational variables, including on/off status ($\boldsymbol{of} \in \{0,1\}^{\boldsymbol{I_{ep} \times T}}$), operating modes ($\boldsymbol{M} \in \{0,1\}^{\boldsymbol{I_{ep} \times T}}$), on/off number ($\boldsymbol{of\_num} \in Z^{\boldsymbol{I_{ep} \times T}}$), input and output power ($\boldsymbol{P_{in}} \in R^{\boldsymbol{I \times T}}, \boldsymbol{P_o} \in R^{\boldsymbol{I \times T}}$), as well as the storage level of storage technologies ($\boldsymbol{SOC} \in R^{\boldsymbol{I_{ST} \times T}}$), and the imported electricity and gas energy ($\boldsymbol{P_{ele}} \in R^{\boldsymbol{T}}, \boldsymbol{P_{gs}} \in R^{\boldsymbol{T}}$).

iii. Auxiliary variables, which are used to linearize non-linear terms, and to combine design variables and operational variables ($\boldsymbol{Ax} \in R^{\boldsymbol{I_{ep} \times J \times T}}$).

3.2 Bounded constraints

In the MILP formulation, the constraints of the problem in this study are described as four categories, technical constraints, operational constraints, economic constraints, and power balance constraints. Here, only the storage system and power balance constraints are given, the rest of constraints can be found in the section 3.1.2 of the supplementary material.

- Storage system

The energy storage system (ESS) in this study is divided into two categories, namely the coupled and decoupled ESS, which are represented by the battery and LAES and their respective models.

- Coupled battery model

The coupled battery model considers the storage as a whole, and its constraints are expressed as in eq. (4) – (5).

$$E_{bat}(t) = E_{bat}(t-1) + \eta_{cha} \cdot P^{-}_{cha,bat} \cdot \Delta t - \frac{P^{+}_{dis,bat} \cdot \Delta t}{\eta_{dis}} \quad (4)$$

$$E_{bat,min} \leq E_{bat}(t) \leq E_{bat,max} \quad (5)$$

where, E – the stored energy (kWh), η – efficiency, Δt – the time interval, the subscripts including: bat – battery, cha – the charging process, dis – the discharging process, max – the maximum value, min – the minimum value, the superscripts including: '-' the input power into storage, '+' the output power from storage. Thermal storage is modelled in a similar way (Steen et al., 2015), but with different parameters.

- Decoupled LAES model

The decoupled LAES model includes the major models of the compressors, turbines and air tanks. The relationships between air mass flow rate, pressure, and power input/output of compressors and turbines are linearized to keep the linearity of MILP formulation. The ramp-up and ramp-down rate, as well as the minimum online and offline time of compressors and turbines are formulated in a similar way to those of gas engines.

Compressors

$$P_{\mathrm{C}}(t) = k_{\mathrm{C}} \cdot \dot{m}_{\mathrm{C}}(t) + C1 \quad (6)$$

$$0 \leq P_{\mathrm{C}}(t) \leq of_{\mathrm{C}}(t) \cdot P_{\mathrm{C},r} \quad (7)$$

Turbines

$$P_{Tr}(t) = k_{Tr} \cdot \dot{m}_{Tr}(t) + C2 \quad (8)$$

$$0 \leq P_{Tr}(t) \leq of_{Tr}(t) \cdot P_{Tr,r} \quad (9)$$

$$0 \leq of_{\mathrm{C}}(t) + of_{Tr}(t) \leq 1 \quad (10)$$

Liquid air tanks

$$m_{LA}(t) = m_{LA}(t-\Delta t) + \dot{m}_{\mathrm{C}}(t) \cdot \Delta t - \dot{m}_{Tr}(t) \cdot \Delta t \quad (11)$$

$$m_{LA,min} \leq m_{LA}(t) \leq m_{LA,max} \quad (12)$$

where, k_{C}/ k_{Tr} – the slopes of the regression curves of compressors/turbines, $C1$ / $C2$ – the intercepts of the regression curves of compressors/turbines, P_{C} / P_{Tr} – the power consumption of compressors/turbines, of_{C} / of_{Tr}– the on-off status of compressors/ turbines, m – the mass

of liquid air in tank, $\dot{m}_C$ / $\dot{m}_{Tr}$ – the air mass flow rates of compressors and turbines, *r*- the rated parameters.

- Power balance constraints

The power and thermal demand and supply should be balanced at each time step, expressed as eq. (13) – (15).

$$P_{GE}(t) + P_{pv}(t) + P_{wt}(t) - P_{cur,wt}(t) - P_{cha,bat}(t) + P_{dis,bat}(t) - P_{cha,C} + P_{dis,Tr}(t) + P_{los}(t) + P_{grid}(t) - P_{HP}(t) - P_{EC}(t) = P_{L,ele}(t) \quad (13)$$

$$P_{HP}(t) + P_{GB}(t) + P_{ht,GE}(t) - P_{cha,ht}(t) + P_{dis,ht}(t) = P_{L,ht}(t) \quad (14)$$

$$P_{EC}(t) + P_{HP}(t) = P_{L,col}(t) \quad (15)$$

where, symbol P – power, the subscripts represent: *GE* – gas engine, *pv* – solar panels, *wt* – wind turbines, *los* – the loss of power, *grid* – the grid electricity, *HP* – heat pump, *EC* – the electric chiller, *L* – load, *ele* – the electricity, *ht* – the heating, *col* – the cooling, *cur*- the curtailed wind, *t* – the time *t*.

3.3 Optimization objectives

The study aims to minimize the total annual system cost and environmental impact, expressed as in eq. (16). The objective terms include: the equipment capital cost $C_{cpt,tot}$, the operational cost C_{op}, the maintenance cost C_{main}, the CO_2 emission tax C_{CO2}, the renewable curtailment cost C_{cur} and the cost penalty C_{LOP} for loss of power (LOP). At the same time, it manages to increase the renewable penetration by maximizing renewable incentives C_{inc}. Detailed description of each optimization objective can be found in the section 3.1.3 of the supplementary material.

$$min\{C_{ann,tot} = C_{cpt,tot} + C_{op} + C_{main} + C_{CO2} + C_{cur} + C_{LOP} - C_{inc}\} \quad (16)$$

The commercial software, including MATLAB, YALMIP, and Gurobi, are combined to conduct the simulation in 1-h resolution rolling-horizon. The MILP relative gap (between 0.001-0.02) is used as the convergence criteria. The gap range considers the trade-off between calculation complexity and time consumption. The computer is configured with an Intel (R) CPU i5-6500 3.2 GHz (4) and 8 GB RAM. Besides, the scaling and various parameters tuning methods were used to speed up the simulation process.

3.4 The methodology

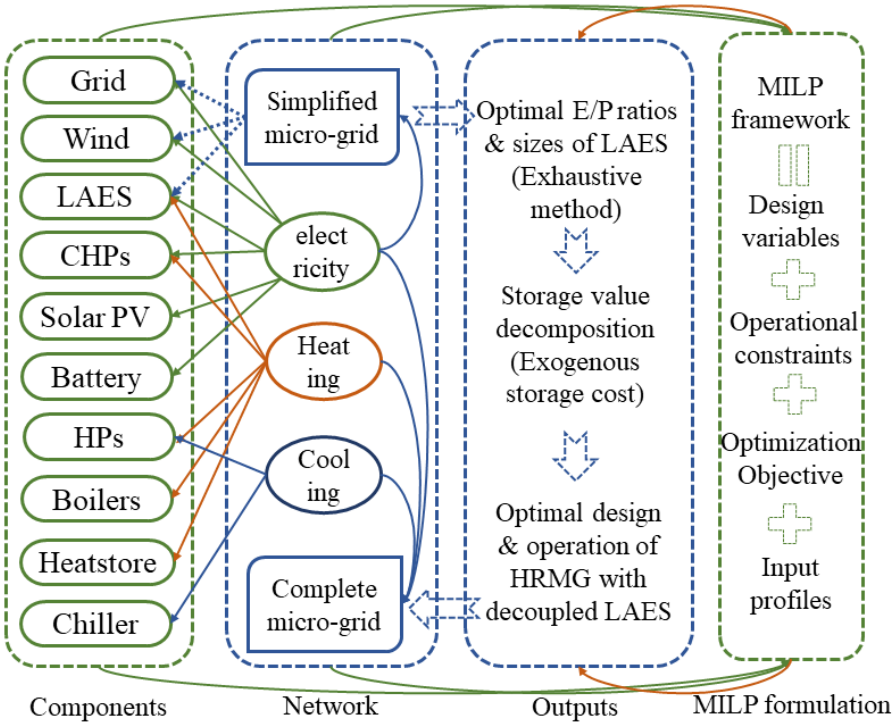

Fig. 4. The methodology and framework of this work

The methodology of the work is shown as in Fig. 4. In the MILP design and operation framework, different system components, such as CHPs, wind turbines, solar panels, heat pumps and heat storage (Heat store) etc., have been included to provide the corresponding energy for different networks (electricity, heating and cooling) within the micro-grid. There are two types of micro-grids developed for the discussion. A simplified micro-grid that only involves electricity network is to study the optimal E/P ratios and sizes of LAES by using exhaustive method. A complete micro-grid involves electricity, heating and cooling networks simultaneously. It is developed to understand the storage value in a comprehensive manner, and eventually to achieve the optimal design and operation of the whole micro-grid.

4 Results and discussions

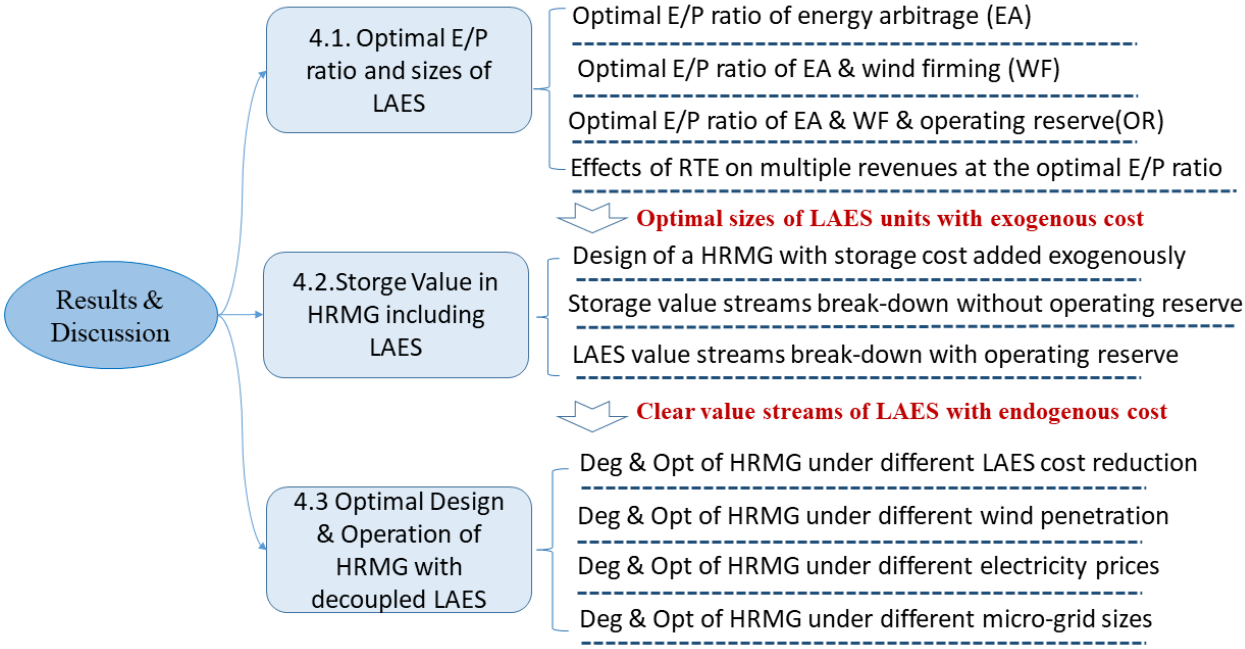

Fig. 5 The logic and structure of discussion part

In this part, the results' discussion is structured as shown in Fig. 5. The optimal E/P ratios and sizes of LAES are obtained by using exhaustive method in section 4.1. Then, the obtained LAES sizes are input into section 4.2, to analyse the storage value with storage cost being added exogenously. After the storage value streams are identified clearly, the optimal design and operation (Des & Opt) of the HRMG with the decoupled LAES and endogenous storage cost can be determined.

4.1 Optimal E/P ratio of LAES

The E/P ratio is the ratio of stored energy (kWh) and rated charge/discharge power (kW), termed as charge/discharge (Cha/Dis) E/P ratios. For the decoupled LAES, when keeping the rated energy capacity (6MWh) constant, increasing charge/discharge E/P ratios results in smaller LFUs and PRUs with higher specific costs and longer working durations. Return on investment (ROI) is the ratio of net profit and investment cost. It is used to quantify the effects of different E/P ratios of LAES on system economics, higher ROI means better cost-effectiveness.

4.1.1 Optimal E/P ratios for energy arbitrage

A simplified micro-grid that only considers the electricity network is assumed as the case study. The LAES is deployed to help conduct the electricity price arbitrage, which is capable of storing electricity at bottom prices and releasing the energy at peak prices to save electricity fee.

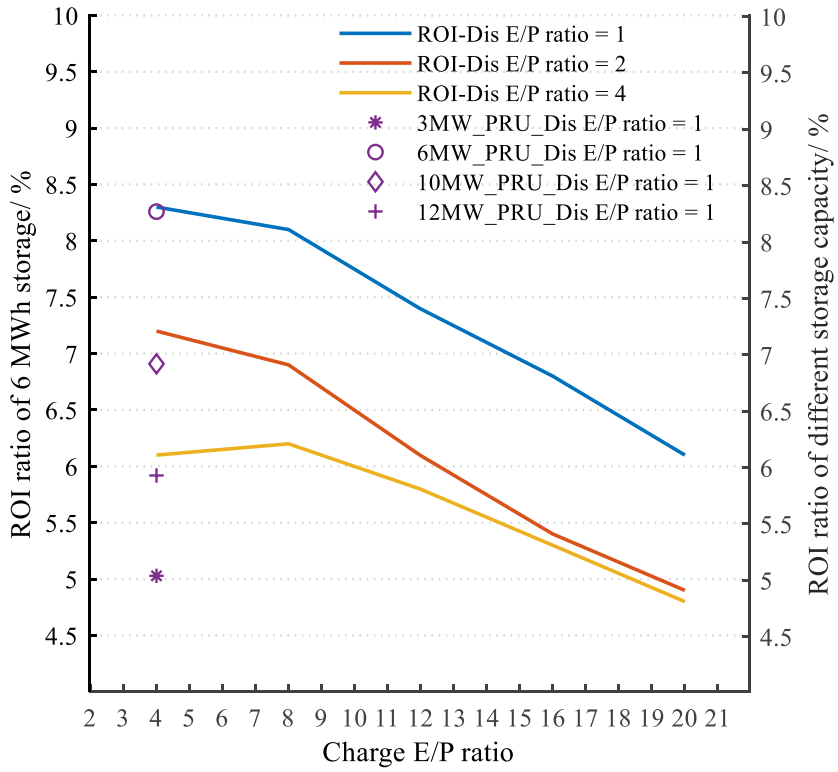

Fig. 6. Effects of different Cha/Dis E/P ratio on system ROI when achieving energy arbitrage

Under different discharge E/P ratios (curves in Fig. 6), the arbitrage revenue and ROI decrease when the charge E/P ratios are more than 4h. It is due to that smaller charging units cannot fully capture the low-price electricity to charge the storage tank to full, though they bear lower capital costs. This results in fewer charge and discharge cycles in a year, thus less arbitrage revenue and lower ROI. While larger discharging units are preferred to capture the highest prices to release the stored electricity and to save more electricity fee, but their specific capital costs are far lower than those of charging units. Indicated by four marks in Fig. 6, keeping the charge/discharge E/P ratios (4/1) constant, the ROI goes up first and then decreases when the sizes of LFU and PRU increase with higher energy capacity of LAES (3 / 6 / 10 / 12 MWh). It can be explained as the value of LAES in the micro-grid has been saturated, the capital cost of the larger-scale storage cannot be offset by its revenue. In other words, there exists the optimal sizes of charge/discharge units and storage capacity of LAES for a given-scale micro-grid, which can achieve good cost-effectiveness.

4.1.2 Optimal tank sizes for energy arbitrage

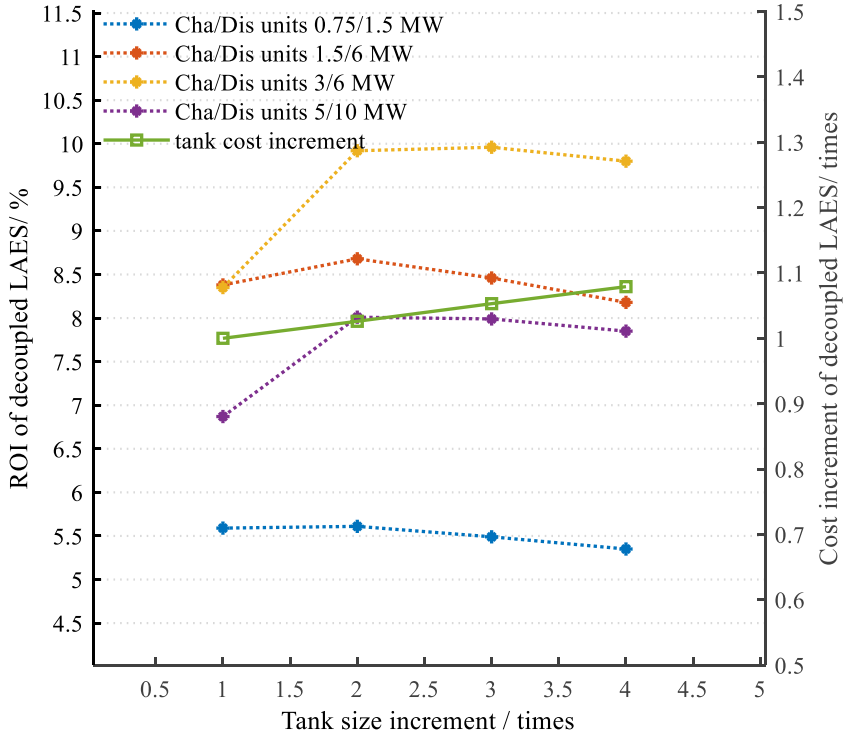

Fig. 7. The effects of tank sizes on system economics

The effects of tank sizes (tons) on system economics were studied as well when keeping the sizes of liquefiers and turbines constant, shown in Fig. 7. Take 3MWh, 6MWh, and 10 MWh of LAESs as the cases, the matching tank sizes can only hold the liquid air produced by LFUs during the rated charging hours (the rated charging E/P ratio). Fig. 7 shows that there exists an optimal tank volume for LAES with specific sizes of liquefiers and turbines, which is two to three times of the matching tank size. It is due to that much larger reservoir cannot be filled to full in the charging process. Thus, the extra investment on larger storage space cannot be counterbalanced by its extra arbitrage profits, which is consistent with the results of Andrea (Vecchi et al., 2020b). Together with the results in section 4.1.1, in terms of arbitrage function provided by LAESs, the discharge power at about half of the maximum electricity demand of micro-grids produces better ROI. Accordingly, the storage system presents the optimal charge E/P ratio (8~12 h) and discharge E/P ratio (2~3 h).

4.1.3 Optimal E/P ratios for wind firming

When the assumed and simplified micro-grid is powered by wind energy (about 50%) and electricity from the grid, the LAES plant is deployed to help achieve wind stabilization. The benefit earned by the LAES is defined as the sum of the avoided curtailment penalty and wind power incentives, the ROI curve is shown in Fig. 8.

It can be seen that it is not favored to choose a larger PRU when keeping LFU size (3 MW) constant (the left bar group), as it contributes less to absorb extra wind power, but results in the decrease of arbitrage revenue and ROI. Further, it is due to that the turbines work more often at part-load conditions to avoid wind curtailment, thus cannot fully capture the peak-price

electricity to release more stored power and reap more profits. However, if keeping the PRU and matching tank size constant, larger LFUs help absorb more wind power, to avoid wind curtailment and increase arbitrage benefits as well (the middle bar group). It is due to that more free wind energy can be captured quickly by larger LFUs and then stored in the form of liquid air, but higher capital costs of larger LFUs worsen the system economics (blue curve in Fig. 8) . Meanwhile, if the matching tank sizes are enlarged by 2-3 times, more extra wind power can be captured and more arbitrage profits can be reaped (the right bar group: ROI 12.4% (matching tank size) to ROI 18.9% (3 times of tank size)). However, an even larger tank (4 times) cannot be charged to full and produce more benefits due to the intermittency of wind energy. Thus, for a LAES with 3 MW LFU and 3MW PRU, the optimal charge and discharge E/P ratios are 12 and 6 h when used for wind firming.

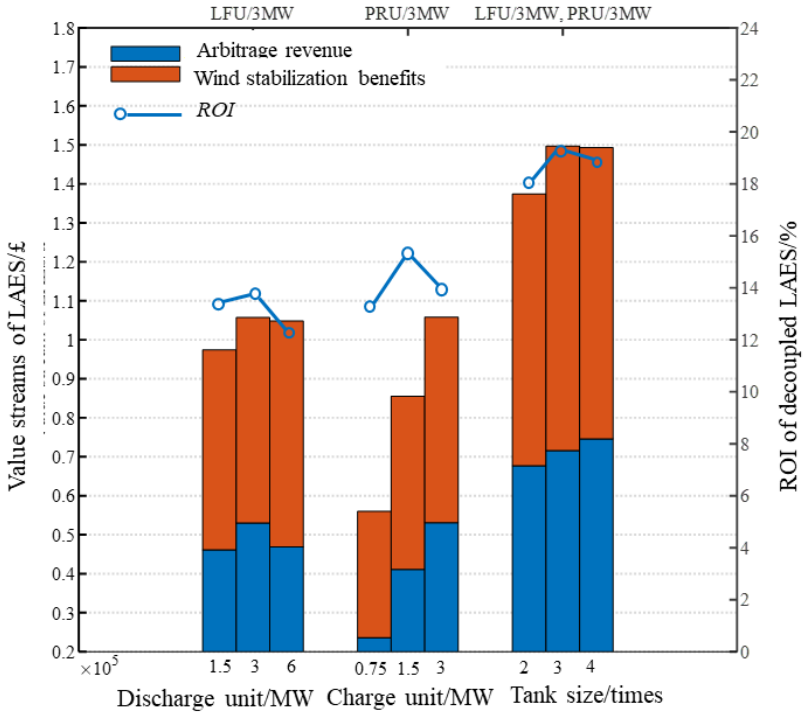

Fig. 8. Effects of Cha/Dis E/P ratio on LAES revenue and ROI when wind curtailment occurs

4.1.4 Optimal E/P ratios for operating reserve

LAES can serve as the secondary upwards reserve (capacity margin for upward regulation) (Luo et al., 2015). The reserve benefits of LAES is assessed by comparing the avoided penalty of loss of power between systems with and without the operating reserve.

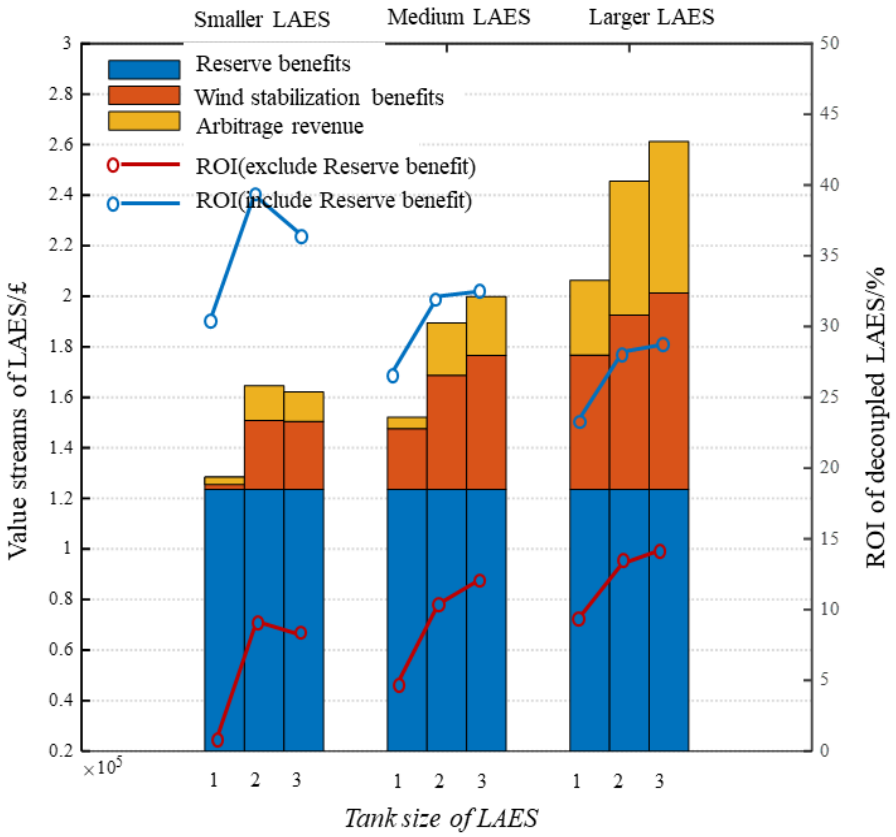

Fig. 9. Total revenue of LAES with different Cha/Dis E/Pratio

The effects of different sizes of LAES plants, namely smaller (0.6/3 MW LFU/PRU), medium (3/3 MW LFU/PRU), and larger (3/6 MW LFU/PRU) ones, on three revenue streams are studied (shown in Fig. 9). It can be seen that the reserve benefits (a major revenue source) of the LAES are not affected by the increasing capacities of units (blue bars from left to right), as the required reserve level can always be met by adjusting the charge and discharge durations (smaller units is charged for longer charge durations, while larger units for shorter charge hours). But the benefits from wind firming and arbitrage are boosted instantly with units' sizes being enlarged (orange and yellow bars from left to right), as larger LAES units are capable of absorbing more low-price electricity and wind energy to keep the reserve level (the LAES capacity is reserved to be no less than 15% of electricidy demand). This leads to more environmental benefits but also higher capital costs, further worse system economics (the blue curves). Thus, in the simulated case, the medium LAES (the middle bar group: 3/3 MW LFU/PRU, Cha/Dis E/P ratio 12/6 h) are chosen to balance the cost-effectiveness and to increase the percentage of wind power as well.

4.1.5 Effects of LAES efficiency on the E/P ratio

In the above cases, the nominal RTE of the LAES is 0.52 under the assumed conditions, but there is still much headroom for the efficiency improvement. Thus, the effects of RTE of the LAES (3/3 MW LFU/PRU, Cha/Dis E/P ratio 12/6 h), improving from 0.5 to 0.6 and 0.7 (Tafone et al., 2019), on the value streams are studied in this work (shown in Fig. 10). It suggests that the reserve revenue (blue bars) is not influenced by the efficiencies, but the

arbitrage revenue (yellow bars) instantly benefits from higher efficiencies of the LAES. It is due to that less electricity needs to be bought from the grid, while more power can be released by PRUs to make the most of price differences. But for higher efficiencies, wind firming revenue decreases slightly (orange bars), because the storage level of liquid air tank increases quickly to full, the spillage of wind energy occurs. Overall, 10%-20% of efficiency improvement results in nearly 2%-3% of enhancement in economics. One of the reasons lies in the lower working RTEs of the LAES, which are 41.8% (rated RTE: 52%), 47.9% (rated RTE: 60%) and 56.9% (rated RTE: 70%) respectively. The PRUs normally work under off-design conditions to provide enough operating reserve, as well as to avoid wind curtailment.

Based on the exhaustive analysis in section 4.1, the cost-effective sizes of LAES units for the specific micro-grid are determined preliminarily to achieve higher ROI. The sizes are 3 MW LFU and 3 MW PRU, as well as the optimal charge and discharge E/P ratios are 12 h and 6 h, and the rated RTE is 0.6.

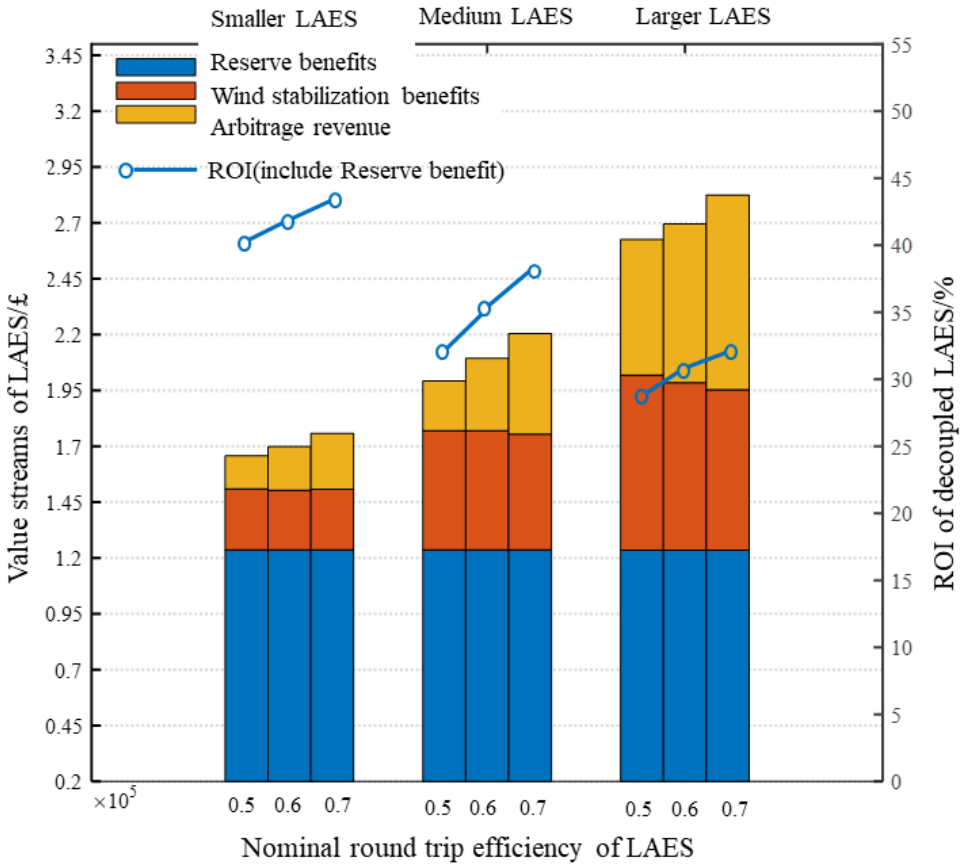

Fig. 10 Effects of LAES nominal efficiency on economics

4.2 Optimal design of a micro-grid and energy storage value

In this section, the benefits (value) of LAES, battery storage, and heat storage in a complete micro-grid with various generators is discussed. To be noted, the capacities and costs of LAES and battery are added to the system exogenously before their value streams are fully understood. The model has been validated by comparing the results with S. G. Sigarchian's (Ghaem Sigarchian et al., 2018). The author adopted the PSO (particle swarm optimization) algorithm to determine the optimal sizes of major components in a poly-generation system.

The results' comparison was shown in Table 4, which confirmed the validity of the MILP design framework in this study. The reason why there is a big difference in the sizes of electric chillers is that the capacities of candidate chillers in the MILP algorithm are in discrete form (200 kW, 500 kW, 800 kW), 3 chillers with 500 kW each were chosen after the MILP optimization.

Table 4. Optimization results comparison

Major system units	Capacity by PSO algorithm	Capacity by this MILP algorithm
CHP unit kW	1000	1000
Boiler kW	2721	3000
Electricity from/to grid kWh	100	113
Electric chiller kW	1100	1500
Heat storage kWh	3000	3000

4.2.1 Optimal design of a micro-grid with storage

To achieve the optimal design of a micro-grid, five basic system scenarios are developed and compared, of which candidate equipment is given in Table 5 and the design result is shown in Fig. 11.

Table 5. System components candidates

System components	0#	1#	2#	3#	4#	5#
grid	✓	✓	✓	✓	✓	✓
gas boilers	✓	✓	✓	✓	✓	✓
electric chiller	✓	✓	×	×	×	×
gas engines	×	✓	✓	✓	✓	✓
heat pumps	×	×	✓	✓	✓	✓
solar PV	×	×	×	✓	✓	✓
wind power	×	×	×	✓	✓	✓
heat storage(HS)	×	×	×	×	✓	✓
LAES	×	×	×	×	×	✓

0 # system is the conventional campus energy system, 1# system is the existing energy system after 2016, 2# ~ 5# systems are newly-developed hydrid renewable energy system. From Fig. 11, solar panels cannot be chosen after the optimization due to the scarce solar energy resource in the UK and its high capital cost. Comparing 1 # and 2 # systems, if electric chillers and part of gas boilers are replaced by reversible heat pumps (HPs), the total annual cost decreases by 18.7%, in which the fuel cost and CO_2 tax drops by 17.7% and 8.2% respectively due to the higher efficiency of HPs (averagely 2.83). Comparing 2 # (comparison base), 3 # and 4 # systems, more wind penetration adds more system capital cost by 37.5% (3 # : wind 17.8%) and 56.2% (4 # : wind 33.74%). But the respective fuel costs and CO_2 emissions declined by 16% ~ 25% and 15.6% ~ 26.2%, the total system annual costs descend by 2% and 4.6% (taking wind and heat incentives into account). If LAES is added into the system (5#

system), the wind power percentage can be further increased to 47% with less curtailment. Correspondingly, the fuel cost, total annual cost and total CO_2 emissions of 5# system can be cut down by 46.6%, 34.7% and 41.5% when compared with those of 1# system. Overall, it indicates the economic and environmental benefits of distributed renewable energy systems with heat pumps, wind power and energy storage technologies. The specific storage value will be discussed in section 4.2.2.

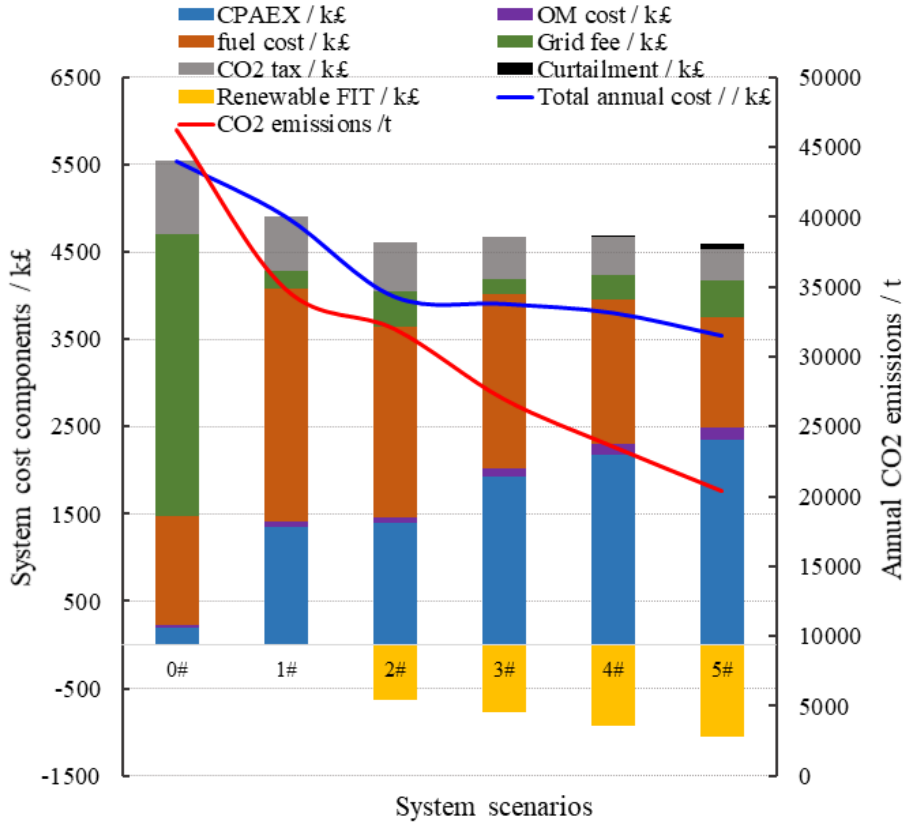

Fig. 11. Cost comparison of different system scenarios

4.2.2 Value of storage in a micro-grid without operating reserve

When wind penetration reaches about 47% (5# system), the effects of heat storage (6MWh), LAES (6 MWh), and battery storage on system annual cost were discussed. A particular focus is put on the benefits analysis of LAES, the value break-downs of each storage are given in Fig. 12.

From the left pie chart in Fig. 12, large heat storage helps achieve about 1.65% of the annual cost reduction, presenting the high ROI (8.19). Specifically, it saves the fuel cost by 29.2%, reduces the captital cost of peak gas boilers by 11%, as well as boosts the heat incentives by 59.8% when working with heat pumps. When LAES is deployed into the micro-grid, the revenues it creates augment with the increase of wind power percentage (from 17.8% to 33.74% to 46.9%). Take the system with 46.9% of wind penetration as an example, the annual revenue of LAES reaches up to k£ 593, corresponding to 74.7% of its annual amortized cost (not taking the operating reserve into account). The whole benefit can be split into five major revenue streams and their respective percentages, illustrated by the middle pie chart in Fig. 12. They

include: the arbitrage revenue (19.85%), wind stabilization benefits (13.82%), peak units saving (33.74%), flexibility value (25.33%) and waste heat benefits (7.27%).

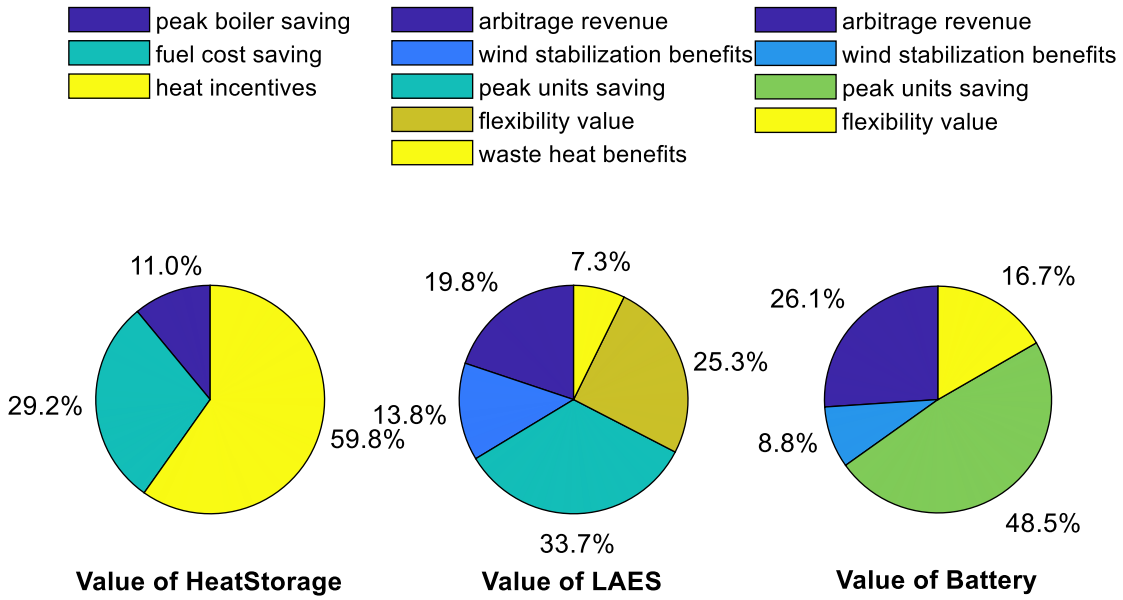

Fig. 12 Value decomposition of three storage technologies

To be more specific, the arbitrage revenue is to fully utilize the spot electricity price differences to save electricity cost. Wind-firming benefit can absorb excess wind energy because of its large storage tank, reducing the wind curtailment by 52.84%. Peak units saving (peak-shaving gain) means the 3MW of LAES discharge unit can replace the 2MW of peak gas engine when the extremely high demand occurs, saving the investment cost of peak gas engines (the biggest revenue source of LAES). To respond to wind variation quickly and accommodate more renewables, several small gas engines with higher specific costs (system without LAES) are required to meet the flexibility requirement. These engines can be replaced by a large gas engine with lower specific cost when the system is equipped with LAES to provide flexibility, leading to another significant cost saving, termed as the flexibility value of the LAES. Besides, if excess compression heat of LAES is utilized to provide heating energy for the HRMG, it helps save one peak gas boiler (1MW) and the corresponding fuel cost, as well as the carbon emissions from boilers. The effects of the LAES on the HRMG is illustrated in Fig. 13, in which the wind curtailment reduction, peak-shaving gain and flexibility value are clearly shown.

Battery storage can achieve the similar functions as those of the LAES in micro-grids except for providing waste heat energy. The value contributions of battery are decomposed as arbitrage revenue (26.1%), wind stabilization benefits (8.8%), peak-shaving gain (48.5%) and flexibility value (16.6%), as shown in the right pie chart in Fig. 12. Its value streams differentiate from those of LAESs, because of the higher efficiency and self-discharge rate of the battery storage, as well as its quick response and no storage tank. Overall, the total value of LAES is higher than that of battery storage by 8.2% when the same investment was made.

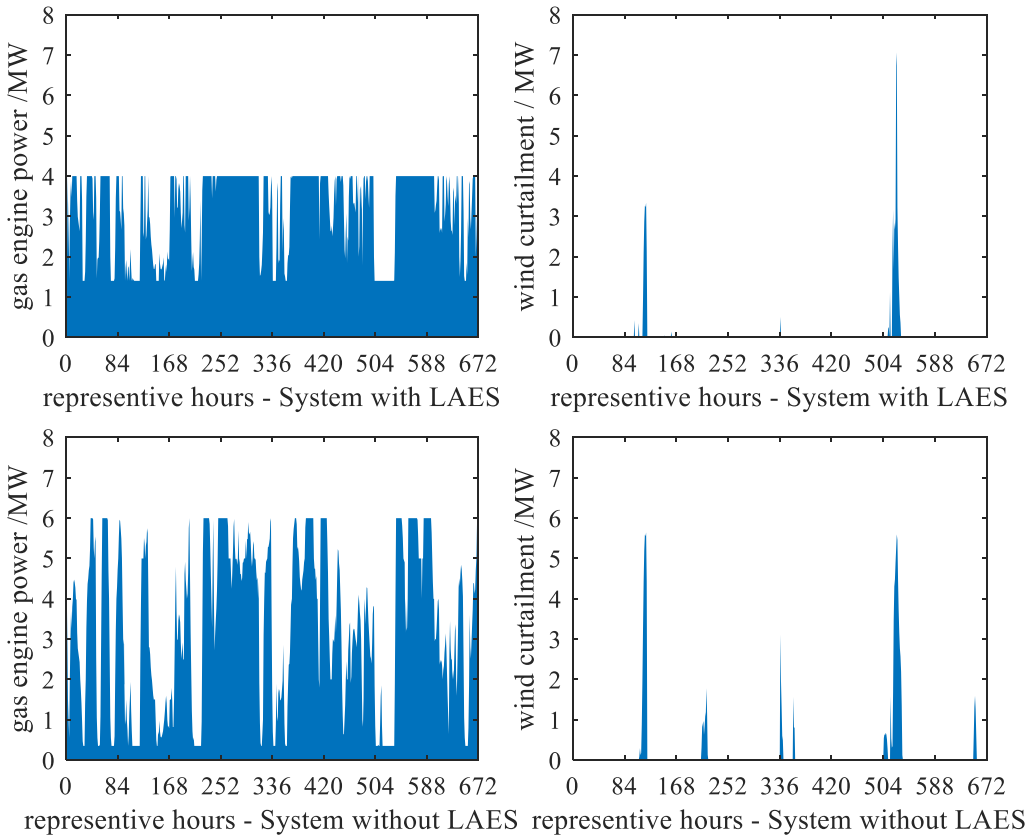

Fig. 13. LAES effects on gas engine output and wind curtailment

4.2.3 Value of LAES in a micro-grid with operating reserve

When LAES is deployed into the micro-grid considering the operating reserve, part of capacities of LAES and gas engines serve as the reserve margins, which is the scheduled output to ensure the robust operation of the system when emergencies occur.

When there is no electric storage, a larger gas engine (5 MW) is equipped to supply electricity and operating reserve simultaneously, resulting in a quite high investment cost of gas engines. However, if the LAES provides part of the reserve capacity, its total value can be augmented by 24.6%, shown as in Fig. 14. Specifically, the arbitrage revenue of the LAES is reduced by 19.6% to 13.2% when providing part of the operating margin. But in return, the size of the gas engine shrinks to 4 MW, of which capital and fuel cost are cut down by 17% and 45.8% respectively, transferring into the reserve value of the LAES (up to 20.4% of the total value). By now, the stacked revenue of the LAES in the micro-grid reaches up to k£ 715.9 when serving as the operating reserve as well, equivalent to 90.2% of its annual amortized cost. Thus, it is believed that the proper investment of LAESs in micro-grids will be increasingly attractive when more renewables and less CO_2 emissions are required, as Herib Blanco *et al.* (2018) argued small storage leads to large benefits.

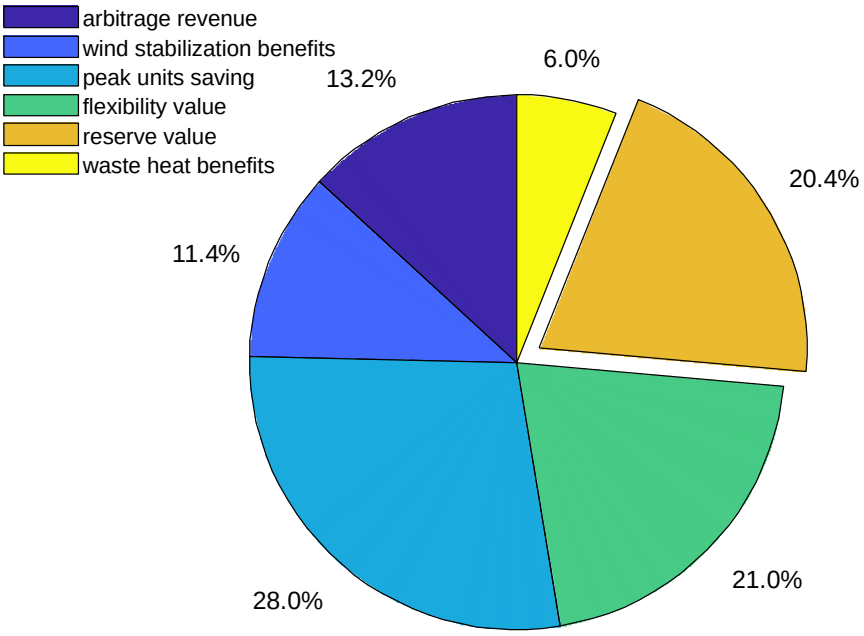

Fig. 14 Value of LAES serving as an operating reserve in micro-grid

4.3 Optimal design and operation of a micro-grid with LAES

In section 4.1 and 4.2, the key benefits and specific value streams of LAESs are fully recognized. In this section, the optimal sizes of the LAES in the HRMG are determined endogenously, together with the determination of other generators' capacities at different scenarios. To be highlighted, only a component is of great value can it be selected in the MILP optimization, which aims at achieving the minimum cost and environmental impact.

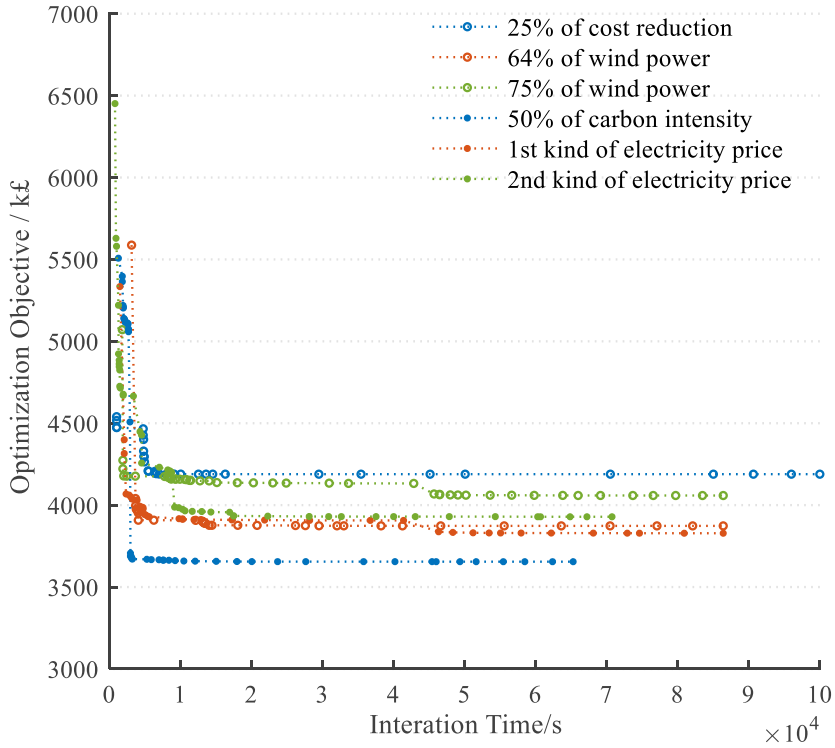

Fig. 15 MILP optimization iteration curve

To be noted, in this section, the convergence criteria differ from those in section 4.1 and 4.2 (MIP gap = 1%). Here, three criteria, namely the Time_Limit >= 24h (864000s), Node_Limit >=120000, MIPgap = 2% were set. The optimization terminates when the first convergence criterion is met, which mainly considers the trade-offs between the solving time and the possible best solution. It is supposed that the objectives achieve the optimum when feasible integer solutions don't update further for enough long time (> 10 h), the converging curves are shown as in Fig. 15.

4.3.1 Effects of the cost reduction of LAES on system design

It is expected the capital cost of LAESs will be reduced when they are deployed on a large scale and volume. In a micro-grid with 50% of wind penetration, 15% and 25% of cost reduction cases are studied, to reveal the effects of LAES capital cost on system design, shown in Table 6. As can be seen, the optimal sizes of the LFU and PRU of the LAES are 3 MW and 3.75 MW respectively. The optimal charge and discharge E/P ratios are 10.4~14h and 5~6.7 h, which is consistent with the exhaustive analysis in section 4.1 and 4.2. It indicates the marginal cost reduction of LAESs does not affect the size selection of LFUs and PRUs, as well as the sizes of other system generators. It is due to that the storage value saturates when its size reaches a specific level in a specified micro-grid. Thus, it does not need larger sizes of LFUs and PRUs when considering economics. But the LAES storage tank size increases from 145 t to 197t, as it can help absorb more wind energy, and reduce wind curtailment and the grid fee, which is profitable and preferable.

Table 6. Optimal design & operation of micro-grid with LAES cost reduction

LAES cost reduction	Engines /MW	WT /MW	Grid /%	HP /MW	Boiler /MW	HS /MWh	LFU /MW	PRU /MW	Tank /tons	System annual cost/k£	LAES annual investment /k£	CO_2 reduction on 2016 level
15%	4	14.63	13.82	5	9	6	3	3.75	145	4277	706.9	41.2%
25%	4	14.60	13.48	5	9	6	3	3.75	197	4190	641.5	41.3%

4.3.2 Effects of a higher wind penetration on system design

Table 7. Optimal design & operation of micro-grid with increasing wind penetration

Wind power %	Engines /MW	WT /MW	Grid /%	HP /MW	Boiler /MW	HS /MWh	LFU /MW	PRU /MW	Tank /tons	System annual cost/k£	LAES annual investment/ k£	CO_2 reduction on 2016 level
64%	2	19.8	20	8	9	10	3	5.2	355	3873.3	729.2	54.6%
75%	1	23.5	20.2	8	11	10	4.8	5.4	605	4058.7	958.6	61.9%

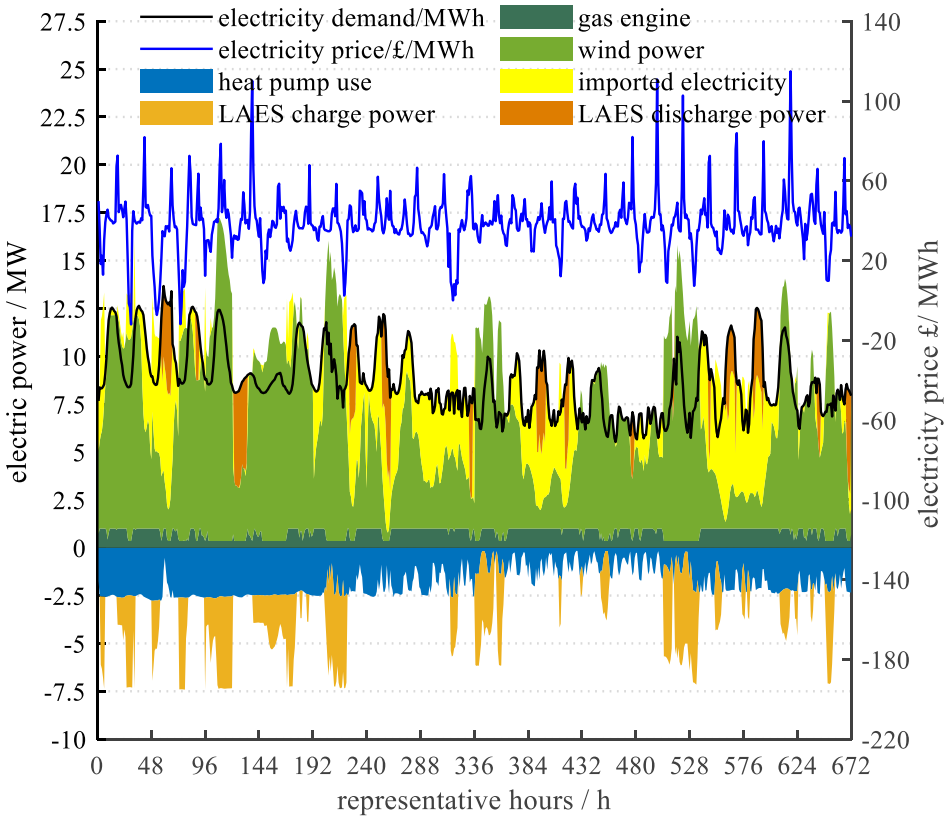

Fig. 16. Optimal power dispatch of the micro-grid with De-LAES and more wind power

In this part, two scenarios of wind penetration (64% and 75%) are studied respectively when 25% of LAES cost reduction is assumed, the results are given in Table 7 and Fig. 16. It is concluded that more wind power percentage is the major driving force to increase the attractiveness of LAES in the micro-grid. From Table 7, the annual investment cost of the LAES increases from k£ 729.2 (64% of wind power) to k£ 958.6 (75% of wind power), as only the value it creates is higher than its investment can the LAES be selected. After the system optimal design, more wind penetration leads to the decrease of gas engines' capacities, as well as the increases in the sizes of LFU, PRU and the tank of the LAES, to absorb and store more wind energy. The rest of power demand is met by purchasing electricity from the grid. As shown in Fig. 16, the LAES mainly serves as stabilizing wind energy, shaving peak, providing operating reserve and flexibility. The optimal charge/discharge E/P ratios and storage tank size are 27/14 h and 605t when the wind percentage is 75% in the micro-grid. The total CO_2 emissions are reduced by about 55% and 62% in the two scenarios on the 2016 level.

4.3.3 Effects of higher electricity prices on system design

In this part, the future grid scenarios are considered, the carbon intensity will drop by 50%, and the electricity prices will go up by 20% and 40% respectively on 2016 level (M, 2018). It is mainly due to higher prices of fuels and more renewables penetration.

Table 8. Optimal design & operation of micro-grid with future grid scenarios

Electricity price Increase	Engines /MW	WT /MW	Grid /%	HP /MW	Boiler /MW	HS /MWh	LFU /MW	PRU /MW	Tank /tons	System annual cost / k£	LAES annual investment / k£	CO_2 reduction on 2016 level
20%	3	15.35	20.67	8	10	10	3	4.2	255	3828.4	673.6	57.8%
40%	3	16.38	18.73	8	9	10	3	4.5	279	3928.9	686.9	59.3%

From the results in Table 8, when electricity price and price difference both go up, the system relies less on the grid but more on wind power, to cut down the operational cost. For LAES selection, the size of LFU keeps unchanged to avoid much increase in investment cost. But the sizes of PRU and storage tank both increase by respective 7.1% and 9.4%, to capture more electricity price arbitrage opportunities and more excess wind energy. In this scenario, the LAES mainly functions to achieve the electricity arbitrage, peak shaving and operating reserve. In the heating sector, the energy shift from electricity to heat by heat pumps (combined with heat storage) becomes even more active. This is motivated by larger electricity price differences, resulting in the savings on the capital cost of one boiler and the corresponding fuel cost. The system tends to produce more heat and store it when there is low-price electricity and surplus wind energy, and then releases the heating energy to supply heat demand when peak-price electricity comes. Thus, heat pumps with heat storage is also a good way to provide system flexibility and absorb excess wind when there is higher renewable penetration, illustrated as in Fig. 17.

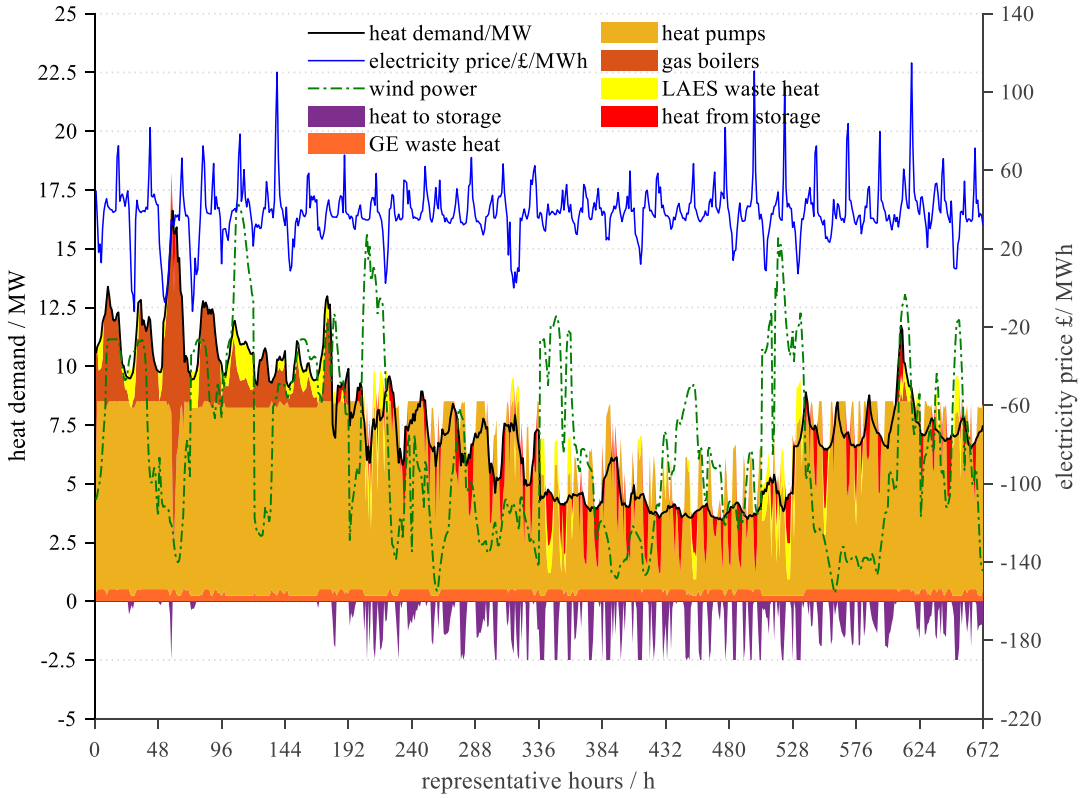

Fig. 17. Optimal heat dispatch of the micro-grid with De-LAES and larger price differences

4.3.4 Effects of different micro-grid sizes on system design

There is currently no clear threshold for classifying the sizes of micro-grids, but most are in the range of 2 ~ 20 MW (Aram, 2020 accessed), few cases can reach up to 50 MW in terms of electric power scale (Julieta Giraldez, 2018). Thus, to discuss the effects of a high demand on the system design and LAES benefits, the campus power demand is assumed to decrease by 50% (representing small micro-grid) and to increase by 50% (representing large micro-grid) on the 2016 level respectively, while keeping at least 50% of renewable power percentage.

Table 9. Optimal design & operation considering different sizes of micro-grids

Micro-grid size/times	Wind power ratio/%	Engines/ MW	WT/MW	Grid/ %	HP/MW	Boiler/MW	HS/MWh	LFU /MW	PRU /MW	Tank/ tons	System annual cost /k£	LAES annual investment /k£	CO2 emissions/ tons
0.5	53.15%	0	10.5	43.8	9	2.5	10	3	3	154	1820.1	612.7	5826.7
1.5	50.5%	6	23.9	13.8	12	15	10	3	7.2	450	5478.6	796.1	20537.3

From Table 9, in a small micro-grid with lower demands, the LAES can even replace gas engines completely and ideally. The results shows that a single LAES plant is multi-functional, which is capable of handling peak shaving and excess wind energy, as well as providing the operating reserve, flexibility requirements and waste heat for the micro-grid. However, in a large micro-grid with higher demands, the capacities of the system equipment all increase significantly to meet higher power and heat demands, including the engines, wind turbines, heat pumps and boilers. For the LAES, the LFU size keeps constant at 3 MW because of its low cost-effectiveness. Another reason lies in the capacity of heat pumps increases by 3MW, which can serve as one way to accommodate more wind energy and provide flexibility for the micro-grid. But the sizes of the PRU and storage tank both increase remarkably, to reduce the capacity of the peak gas engine and to provide enough operating reserve. It is due to there are larger differences between the electricity peaks and valleys, as well as a higher requirement for the operating reserve. This case discussion verifies the robustness of the MILP design framework, which is capable of achieving the optimal design and operation of micro-grids with the decoupled LAES under different application scenarios.

5 Conclusions

In this work, a decoupled LAES energy storage model under off-design conditions was developed, to adapt to variable renewables and user demands. It was then integrated into a MILP design framework of a hybrid renewable micro-grid (HRMG).

Firstly, based upon the framework, the optimal charge/discharge E/P ratios and storage tank sizes of LAES were studied first by using exhaustive method. It indicates that there exist the optimal sizes of LAES units when it provides different services in a HRMG.

Secondly, the benefits of LAES, TES and battery in the HRMG are split into different value streams for the first time. For a micro-grid with 50% of wind power, the LAES in it can

help achieve multiple functions, corresponding to six explicit value streams that can be stacked up. They include: the time shifting (13.2%), renewable firming (11.4%), peak shaving (28%), flexibility (21%) and reserve value (20.4%), as well as the waste heat recovery (6%). The total profit of the LAES is 8.2% higher than that of battery storage with the same investment cost. Other potential benefits of LAESs, like the investment deferral of the network, increasing system stability and avoiding equipment fatigue, as well as stabilizing renewables and other profounding environment benefits will be explored in the further work.

Finally, the optimal design and operation of the HRMG with the decoupled LAES under different scenarios were investigated by the developed MILP framework for the first time. The results indicate the key value of LAESs to support the future HRMGs and its attractiveness in HRMGs, which is mainly motivated by higher requirements on wind power and CO_2 emission reduction. However, there are also limitations, like the grid network expansion was not fully considered, which will be focuses in the next stage. The practical significance of this work lies in it enables the micro-grid operator to preliminarily determine the optimal sizes of system components, as well as the LAES units' sizes under a specific renewable penetration and application scenario, to achieve the optimal deployment and minimize the investment cost and CO_2 emissions.

ACKNOWLEDGEMENT

Ting Liang, Paul A. Webley, and Yulong Ding acknowledge the partial support from Priestley Joint Ph.D. Scholarship from the University of Birmingham (UK) and University of Melbourne (Australia). Thanks to the partial support from UK EPSRC under grants EP/N032888/1, EP/P003605/1 and EP/S032622/1.

REFERENCE:

Alberizzi, J.C., Rossi, M., Renzi, M., 2020. A MILP algorithm for the optimal sizing of an off-grid hybrid renewable energy system in South Tyrol. Energy Reports 6, 21-26.

Aram, A., 2020 accessed. Microgrid Market in the USA. Hitachi Review 66(5), 454–455.

Arcuri, P., Florio, G., Fragiacomo, P., 2007. A mixed integer programming model for optimal design of trigeneration in a hospital complex. Energy 32(8), 1430-1447.

Ayele, G.T., Mabrouk, M.T., Haurant, P., Laumert, B., Lacarrière, B., 2019. Optimal placement and sizing of heat pumps and heat only boilers in a coupled electricity and heating networks. Energy 182, 122-134.

Buonomano, A., Calise, F., Ferruzzi, G., Vanoli, L., 2014. A novel renewable polygeneration system for hospital buildings: Design, simulation and thermo-economic optimization. Appl Therm Eng 67(1-2), 43-60.

de Bosio, F., Verda, V., 2015. Thermoeconomic analysis of a Compressed Air Energy Storage (CAES) system integrated with a wind power plant in the framework of the IPEX Market. Appl Energ 152, 173-182.

Djelailia, O., Kelaiaia, M.S., Labar, H., Necaibia, S., Merad, F., 2019. Energy hybridization photovoltaic/diesel generator/pump storage hydroelectric management based on online optimal fuel consumption per kWh. Sustainable Cities and Society 44, 1-15.

F. J. de Sisternes, M.D.W., 2013. Optimal Selection of Sample Weeks for Approximating the Net Load in Generation Planning Problems. Massachusetts Institute of Technology.

Gabrielli, P., Gazzani, M., Martelli, E., Mazzotti, M., 2018. Optimal design of multi-energy systems with seasonal storage. Appl Energ 219, 408-424.

Geidl, M., 2007. Integrated Modeling and Optimization of Multi-Carrier Energy Systems. ETH Zurich.

Ghaem Sigarchian, S., Malmquist, A., Martin, V., 2018. Design Optimization of a Complex Polygeneration System for a Hospital. Energies 11(5).

Good, N., Martínez Ceseña, E.A., Zhang, L., Mancarella, P., 2016. Techno-economic and business case assessment of low carbon technologies in distributed multi-energy systems. Appl Energ 167, 158-172.

Jihane Kartite, M.C., 2019. Study of the different structures of hybrid systems in renewable energies-A review. Energy Procedia 157, 323-330.

Julieta Giraldez, F.F.-E., Sara MacAlpine, Peter Asmus, 2018. Phase I Microgrid Cost Study: Data Collection and Analysis of Microgrid Costs in the United States.

Lian, J., Zhang, Y., Ma, C., Yang, Y., Chaima, E., 2019. A review on recent sizing methodologies of hybrid renewable energy systems. Energ Convers Manage 199.

Luo, X., Wang, J., Dooner, M., Clarke, J., 2015. Overview of current development in electrical energy storage technologies and the application potential in power system operation. Appl Energ 137, 511-536.

M, A., 2018. BEIS 2018 Updated Energy & Emissions Projections: Growth assumptions and prices. https://assets.publishing.service.gov.uk/government/uploads/system/uploads/attachment_data/file/802478/Annex-m-price-growth-assumption_16-May-2019.ods.

Martínez Ceseña, E.A., Good, N., Syrri, A.L.A., Mancarella, P., 2018. Techno-economic and business case assessment of multi-energy microgrids with co-optimization of energy, reserve and reliability services. Appl Energ 210, 896-913.

Mazzoni S., O.S., 2019. Liquid Air Energy Storage as a polygeneration system to solve the unit commitment and economic dispatch problems in micro-grids applications. 10th International Conference on Applied Energy 158, 5026-5033.

Mokhtara, C., Negrou, B., Bouferrouk, A., Yao, Y., Settou, N., Ramadan, M., 2020. Integrated supply–demand energy management for optimal design of off-grid hybrid renewable energy systems for residential electrification in arid climates. Energ Convers Manage 221.

Nabat, M.H., Zeynalian, M., Razmi, A.R., Arabkoohsar, A., Soltani, M., 2020. Energy, exergy, and economic analyses of an innovative energy storage system; liquid air energy storage (LAES) combined with high-temperature thermal energy storage (HTES). Energ Convers Manage 226.

She, X., Peng, X., Nie, B., Leng, G., Zhang, X., Weng, L., Tong, L., Zheng, L., Wang, L., Ding, Y., 2017. Enhancement of round trip efficiency of liquid air energy storage through effective utilization of heat of compression. Appl Energ 206, 1632-1642.
Singh, G., Das, R., 2021. Experimental study of a combined biomass and solar energy-based fully grid-independent air-conditioning system. Clean Technologies and Environmental Policy 23(6), 1889-1912.
Singh, G.K., Das, R., 2018. Energy Saving Potential of a Combined Solar and Natural Gas-Assisted Vapor Absorption Building Cooling System. Journal of Solar Energy Engineering.
Steen, D., Stadler, M., Cardoso, G., Groissböck, M., DeForest, N., Marnay, C., 2015. Modeling of thermal storage systems in MILP distributed energy resource models. Appl Energ 137, 782-792.
Tafone, A., Romagnoli, A., Borri, E., Comodi, G., 2019. New parametric performance maps for a novel sizing and selection methodology of a Liquid Air Energy Storage system. Appl Energ 250, 1641-1656.
Tu, T., Rajarathnam, G.P., Vassallo, A.M., 2019. Optimization of a stand-alone photovoltaic–wind–diesel–battery system with multi-layered demand scheduling. Renew Energ 131, 333-347.
Vecchi, A., Li, Y., Mancarella, P., Sciacovelli, A., 2020a. Integrated techno-economic assessment of Liquid Air Energy Storage (LAES) under off-design conditions: Links between provision of market services and thermodynamic performance. Appl Energ 262.
Vecchi, A., Li, Y., Mancarella, P., Sciacovelli, A., 2021. Multi-energy liquid air energy storage: A novel solution for flexible operation of districts with thermal networks. Energ Convers Manage 238.
Vecchi, A., Naughton, J., Li, Y., Mancarella, P., Sciacovelli, A., 2020b. Multi-mode operation of a Liquid Air Energy Storage (LAES) plant providing energy arbitrage and reserve services – Analysis of optimal scheduling and sizing through MILP modelling with integrated thermodynamic performance. Energy 200.
Vivien Foster, D.B., 2014. Understanding CO2 emissions Emissions from the Global Energy Sector. The World Bank.
Xie, C., Hong, Y., Ding, Y., Li, Y., Radcliffe, J., 2018. An economic feasibility assessment of decoupled energy storage in the UK: With liquid air energy storage as a case study. Appl Energ 225, 244-257.
Yang, Y., Zhang, S., Xiao, Y., 2015. An MILP (mixed integer linear programming) model for optimal design of district-scale distributed energy resource systems. Energy 90, 1901-1915.
Yokoyama, R., Shinano, Y., Taniguchi, S., Ohkura, M., Wakui, T., 2015. Optimization of energy supply systems by MILP branch and bound method in consideration of hierarchical relationship between design and operation. Energ Convers Manage 92, 92-104.
Zakeri, B., Syri, S., Rinne, S., 2015. Higher renewable energy integration into the existing energy system of Finland – Is there any maximum limit? Energy 92, 244-259.